SUPPORTING INFORMARION

High Brightness Circularly Polarized Electroluminescence from Conjugated Polymer F8BT Induced by Chiral Binaphthyl-pyrene

Xueyan Zhang, [a] Zhaoran Xu,[a] Yu Zhang, [a] Yiwu Quan,*[a] Yixiang Cheng,*[b]

a. Key Laboratory of High Performance Polymer Materials & Technology of Ministry of Education, School of Chemistry and Chemical Engineering, Nanjing University, Nanjing 210023, China. E-mail: quanyiwu@nju.edu.cn

b. Key Lab of Mesoscopic Chemistry of MOE and Jiangsu Key Laboratory of Advanced Organic Materials, School of Chemistry and Chemical Engineering, Nanjing University, Nanjing 210023, China. E-mail: yxcheng@nju.edu.cn.

Contents

1. Thermal Properties of Compounds *R*-3

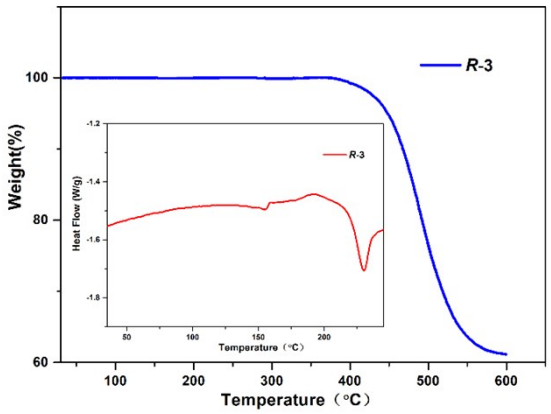

Figure S1. TGA curves of ***R*-3**; Inset curve: DSC curves of ***R*-3**.

2. Chiroptical Properties of Compounds *R*-/*S*-3

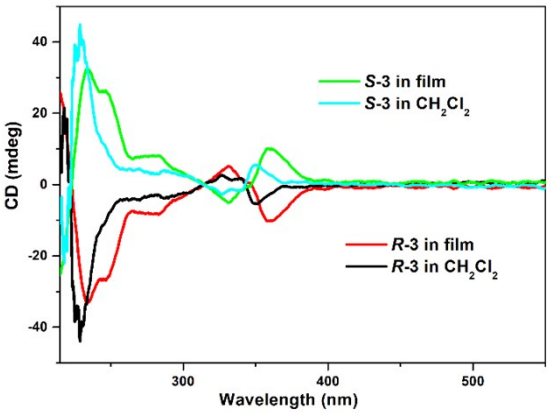

Figure S2 CD spectra of ***R*-/*S*-3** in CH_2Cl_2 (1.0×10^{-5} M) and spin-coated films.

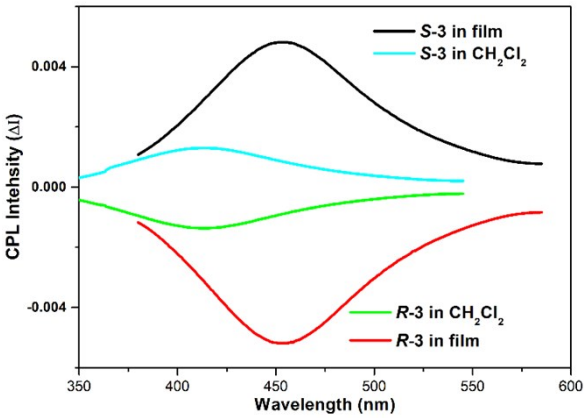

Figure S3 CPL spectra of ***R*-/*S*-3** in CH_2Cl_2 (1.0×10^{-5} M) and spin-coated films.

3. Electrochemical Measurements

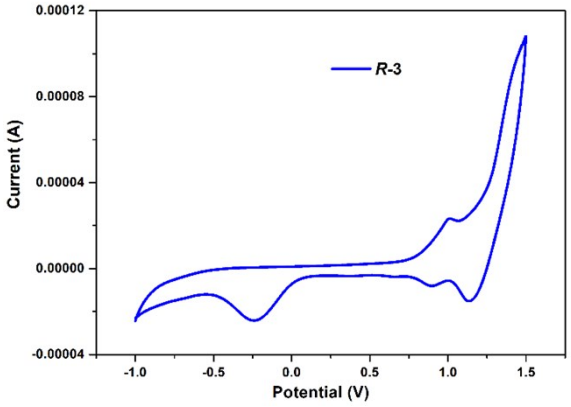

Figure S4 CV curves of ***R*-3** in CH_2Cl_2 solution

Table S1 Electrochemical characteristic properties of compounds ***R*-3**

Compounds	[a]$\lambda_{abs,\ onset}$	[a]E_g	$E_{ox,onset}$	[a]HOMO/LUMO	[b]$\lambda_{abs,\ onset}$	[b]HOMO/LUMO	[b]E_g
	(nm)	(eV)	(V)	(eV)	(nm)	(eV)	(eV)
***R*-3**	380	3.26	1.013	-5.24 /-1.98	390	-5.23 /-1.62	3.61

a: Measured in CH_2Cl_2 at room temperature in the presence of ***R*-3** (0.5 mmol/L), ferrocene (0.5 mmol/L) as an internal standard, and *n*-Bu_4NPF_6 (0.1 M) as an electrolyte; $E_g = 1240/\lambda_{onset,}$ calculated from the absorption edge; $E_{HOMO} = -(E_{ox,\ onset} - E(Fc/Fc^+) + 4.8)$ eV, $E(Fc/Fc^+) = 0.587$ V vs Ag/AgCl; $E_{LUMO} = E_{HOMO} + E_g$; b: Values in parentheses are obtained at the B3LYP-D3(BJ)/6-31G** level.

4. CP-OLED Performances and Electroluminescence Spectra of *R*-/*S*-3

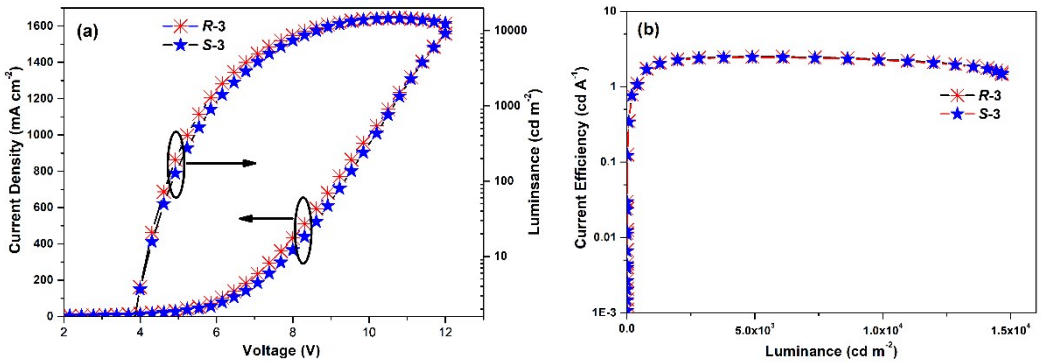

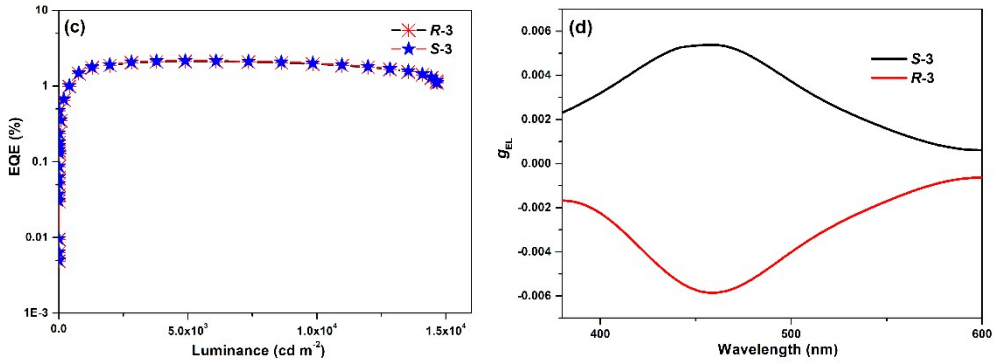

Figure S5 CP-OLED performance of devices based on ***R*-/*S*-3**.

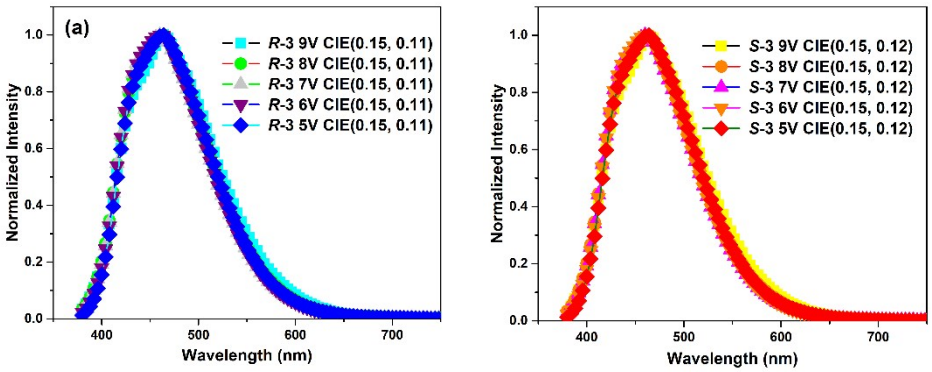

Figure S6 Electroluminescence spectra of devices based on ***R*-/*S*-3**.

5. Photophysical Spectra of F8BT + *R*-/*S*-3

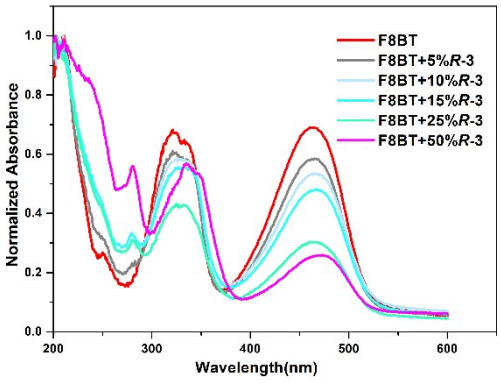

Figure S7 UV-*vis* absorption in spin-coated films of blends system **F8BT** + wt% ***R*-/*S*-3**.

Table S2 Fluorescent quantum yield (Φ_F) of as-cast/annealed F8BT and blends F8BT+***R*-3** films

Sample	Dopant (wt%)	Φ_F (%)
F8BT/as-cast	0	12.6
F8BT + ***R*-3**/as-cast	5	27.8

F8BT + ***R*-3**/as-cast	10	28.5
F8BT + ***R*-3**/as-cast	15	32.3
F8BT + ***R*-3**/as-cast	25	28.7
F8BT + ***R*-3**/as-cast	50	27.6
F8BT/annealed	0	19.7
F8BT + ***R*-3**/ annealed	5	36.6
F8BT + ***R*-3**/ annealed	10	43.5
F8BT + ***R*-3**/ annealed	15	52.7
F8BT + ***R*-3**/ annealed	25	46.3
F8BT + ***R*-3**/ annealed	50	47.3

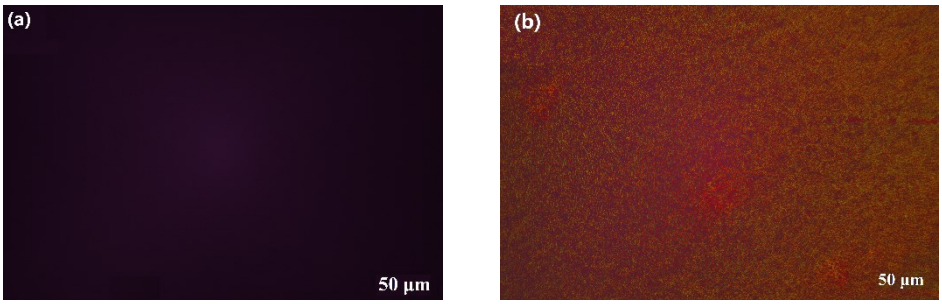

Figure S8 Cross-polarized optical microscope images (100×) of as-cast (c) and annealed F8BT + 10% ***R*-3** films (d).

6. Electroluminescence Spectra of Devices based on blends F8BT + *R*-/*S*-3

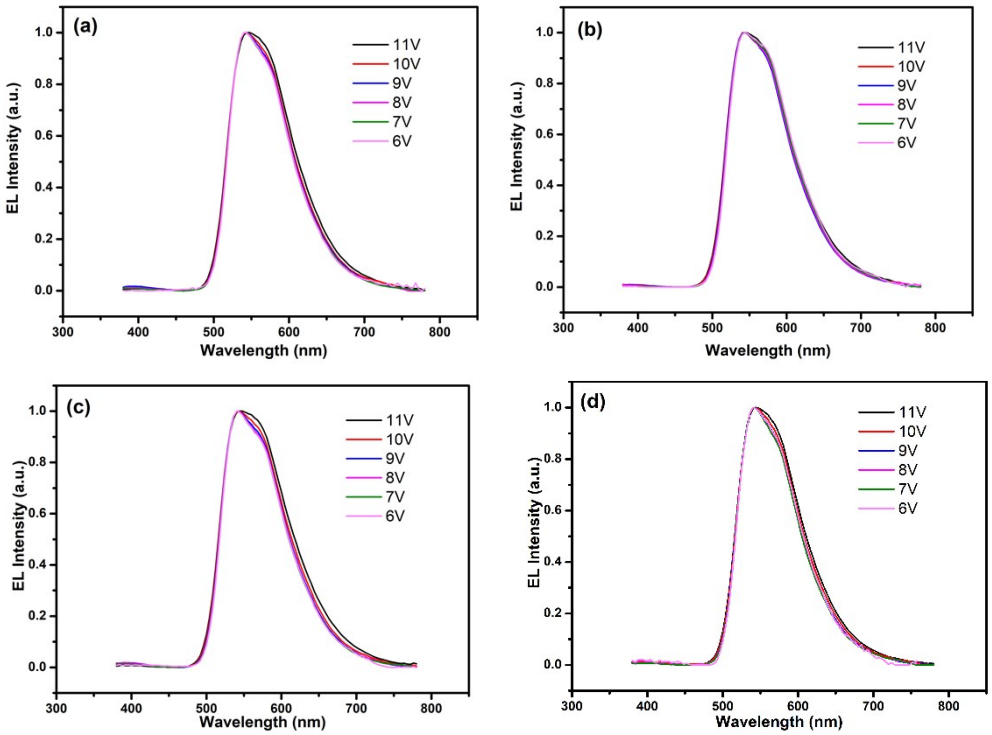

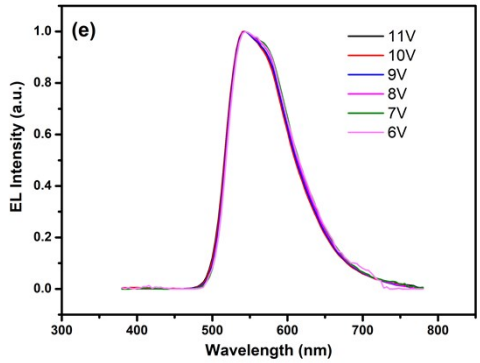

Figure S9 Electroluminescence spectra of devices based on blends **F8BT**+ wt% ***R***-/***S***-**3**; (a) 5% ***R***-**3**; (b) 10% ***R***-**3**; (c) 15% ***R***-**3**; (d) 25% ***R***-**3**; (e) 10% ***S***-**3**.

7. NMR Spectra *vs* MS Spectrum of Compounds

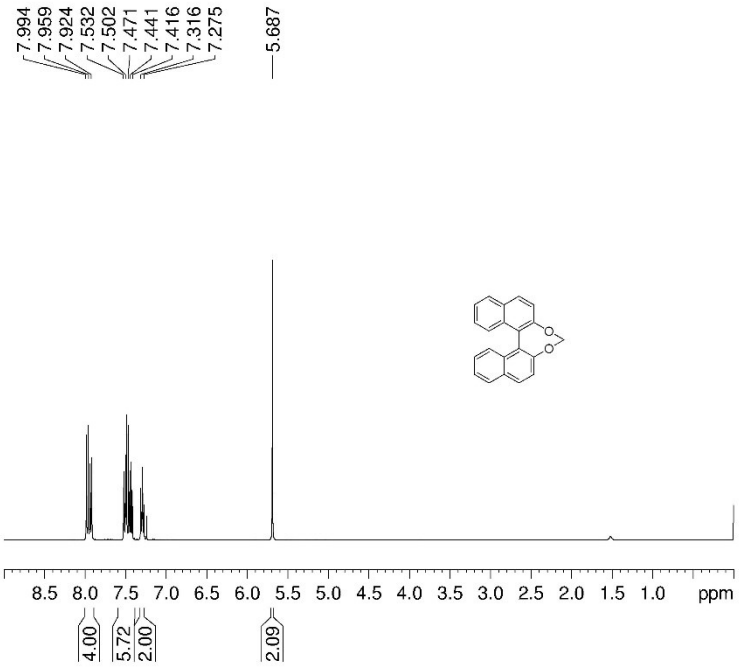

^{1}H NMR spectrum of compound ***R***-**1**

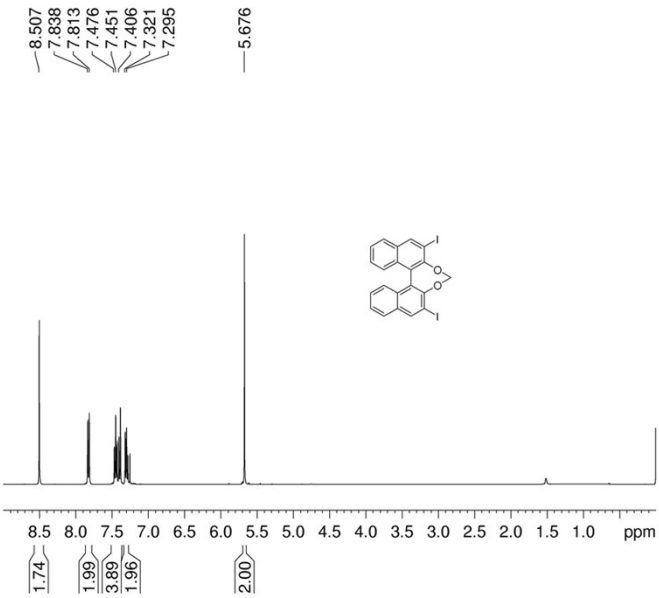

^{1}H NMR spectrum of compound ***R*-2**

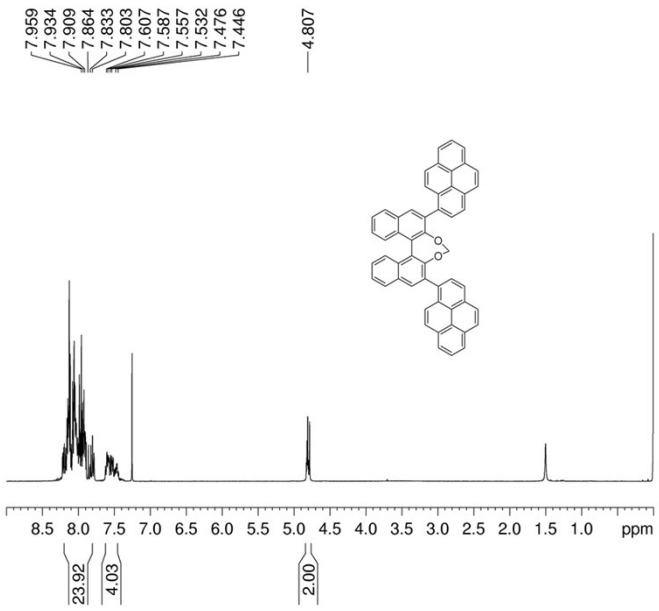

^{1}H NMR spectrum of compound ***R*-3**

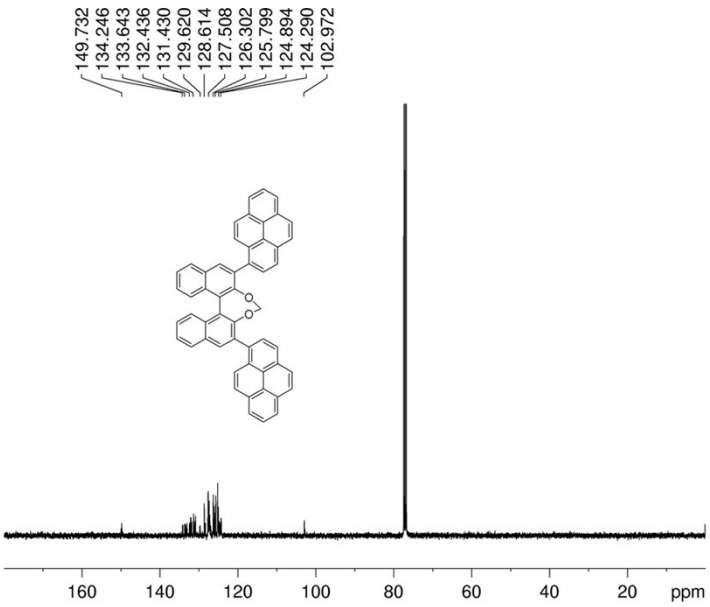

^{13}C NMR spectrum of compound ***R*-3**

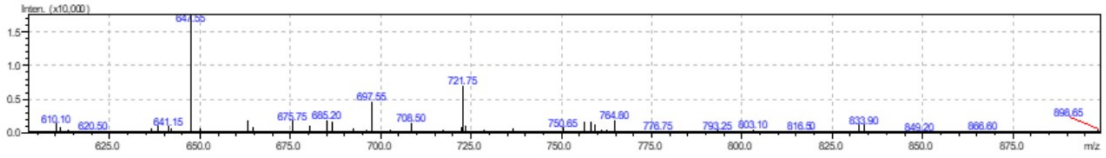

MS spectrum of compound ***R*-3**

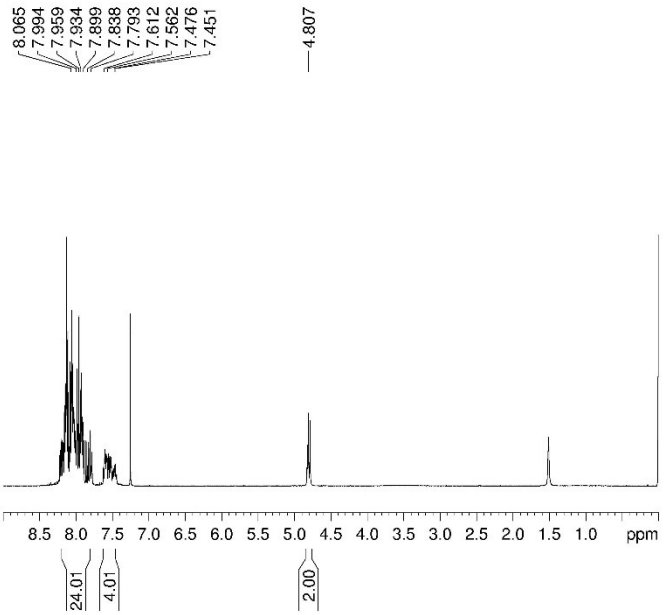

^{1}H NMR spectrum of compound ***S*-3**